J. Phys.: Condens. Matter **12** (2000) 6245–6252. Printed in the UK PII: S0953-8984(00)13395-8

Chemical bond analysis of the second-order nonlinear optical behaviour of Mg-doped lithium niobate

D Xue, K Betzler and H Hesse

Fachbereich Physik, Universität Osnabrück, D-49069 Osnabrück, Germany

E-mail: klaus.betzler@uni-osnabrueck.de

Received 19 April 2000

Abstract. Second-order nonlinear optical properties of Mg-doped lithium niobate single crystals are quantitatively studied from the chemical bond viewpoint. The results show that the second-order nonlinear optical response of Mg-doped $LiNbO_3$ single crystals at 1079 nm decreases linearly with increasing Mg concentration in the crystal. This linear correlation is quantitatively evaluated in the current work.

1. Introduction

For several decades $LiNbO_3$ (LN) has been of great interest for both fundamental science and applications in optics due to its large electro-optical and nonlinear optical (NLO) coefficients [1, 2]. Since LN is a typical nonstoichiometric crystal, it contains specific structural vacancies (i.e., empty oxygen octahedra) [3] and other intrinsic defects in its crystal structure [4, 5]. Therefore, various dopants ranging from the H^+ with valence +1 to the rare-earth cations with valence +3 can be introduced into the crystallographic frame occupying Li sites [6]. This wide range of dopants accounts for the attractive versatility for many important applications [7]. Yet, since there is a serious optical damage problem due to the photorefractive effect in LN optical devices, the search for impurities which are 'optical damage resistant' becomes technologically very important [8]. This damage problem can be greatly reduced by co-doping LN single crystals with MgO at a concentration of about 5% [9, 10].

The defect structure and therewith-related properties of LN have been extensively studied [11, 12]; numerous investigations concerning the lattice sites of dopants and their incorporation mechanisms [6, 13–15] have been performed. It seems to have become clear that the Li vacancy model is reasonable for describing the defect structure of nonstoichiometric LN single crystals [5], and that dopants prefer to occupy Li sites [6, 13]—at least in the low-concentration regime (<6% molar content).

Any changes in the crystal composition will finally affect all corresponding physical properties of LN, causing e.g. changes of the linear dielectric response, i.e., the refractive indices, and changes of the second-order NLO response. Our previous experimental works have shown the important compositional influence of Mg doping in LN samples, grown from congruent melt with up to 9 mol% Mg, on the refractive indices at various wavelengths. The observed results can be excellently described by a generalized Sellmeier equation [16]. The influence of composition on the second-order NLO behaviour of Mg-doped LN single crystals has not been quantitatively investigated to date.

0953-8984/00/286245+08$30.00

Our chemical bond method allows us to derive dielectric responses of crystal materials from corresponding crystallographic structures using the constructed structure–property relationship [17]. In a former work [18], we have quantitatively studied linear and second-order nonlinear optical responses of LN at 1064 nm from the detailed crystallographic structure at room temperature [3]. In the present work, the second-order NLO behaviours of Mg-doped LN at 1079 nm will be quantitatively studied on the basis of the chemical bond viewpoint [17, 19] and the constitution–property relationship for crystal materials [20].

2. Structural characteristics analysed by the bond-valence model

In recent years the electrostatic valence principle has been elaborated into the bond-valence model, an empirical theory that allows a quantitative prediction of the geometry of many inorganic compounds [19]. The theory treats a compound as an infinite network of constituent atoms linked by chemical bonds. For crystals, this can be reduced to a finite network comprising a single formula unit such as the network of $LiNbO_3$, the graph of which is shown in figure 1. Each line represents a different bond, so Li^+ and Nb^{5+} are six coordinated and O^{2-} is four coordinated. Each atom i in the graph is assigned a formal charge equal to its *atomic valence* or oxidation state (V_i) and each bond between atoms i and j is assigned a *bond valence* (s_{ij}). The bond valences are determined by the following two *network equations*:

$$\sum_j s_{ij} = V_i \tag{1}$$

and

$$\sum_{\text{loop}} s_{ij} = 0. \tag{2}$$

In the crystallographic structure of pure LN single crystals, the ideal cation stacking sequence along the c-axis is $\cdots$–Li–Nb–□–Li–Nb–□–$\cdots$, where □ represents a structural vacancy (an empty octahedron) [3]. This ideal stacking sequence (constituent octahedra in pure LN) is sketched in figure 2. However, when Mg^{2+} cations are introduced as dopants into such a stacking sequence, the situation changes to a different case. A Mg ion will substitute for two Li ions occupying a Li site and forming a corresponding Li vacancy (see the planar view of the a–b plane in figure 3). This incorporation of Mg^{2+} at Li sites was discussed by several authors [13, 15, 21–23] and has been experimentally proved to occur [15, 21]. If a few Mg ions substitute for Li (up to about 5 mol%), one will have a corresponding number of Li sites occupied by Mg and an equal number of vacancies. This results in O atoms with different environments. All will have two (5/6) valences from the Nb atoms, but they will have either two bonds to Li (sum at O = 2.00), or one bond to Li and one to Mg (sum at O = 2.17), or one bond to Mg and one vacancy (sum at O = 2.00), or one bond to Li and one vacancy (sum at O = 1.83). Further, it is possible, albeit unlikely, that there are oxygens bonded to two vacancies (sum at O = 1.67). Of course, since the sums at O are now not all exactly 2.00, the structure will relax by strengthening some bonds and weakening others until an equilibrium is reached in which the sums at O are all close to 2.00.

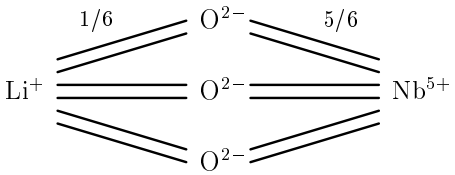

Figure 1. The bond graph of $LiNbO_3$. The valences of atoms and theoretical valences of the bonds are shown. Double lines denote two non-equivalent bonds.

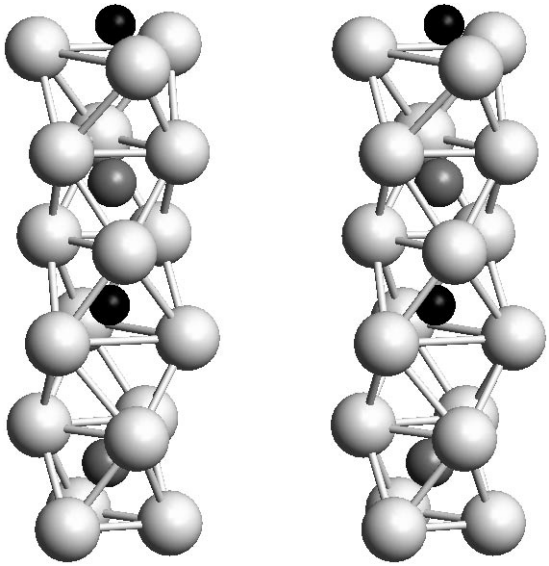

Figure 2. A stereoscopic view (intended to be viewed with crossed eyes) of the ideal crystal stacking sequence of lithium niobate along the crystallographic *c*-axis (light grey: oxygen; dark grey: niobium; black: lithium).

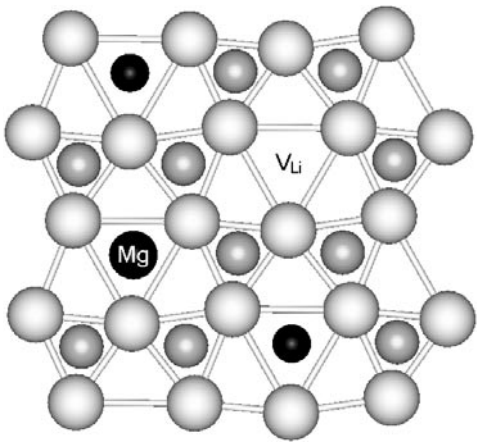

Figure 3. The crystallographic *a*–*b* plane of Mg-doped lithium niobate. One Mg ion replaces two Li ions occupying a Li site and additionally forming a Li vacancy (V_{Li}). Light grey: oxygen lattice; dark grey: niobium; black: lithium or magnesium.

The important criteria for selecting suitable dopants for a given crystal are the size of the atoms (Mg is similar in size to Li and only a little larger than Nb) and the bonding strength (expected bond valence). In the Mg-doped LN single crystals, the sizes are not so different, but the bonding strengths are, so substitution at the Li site gives the least disruption of the bonding framework. Since all the cations in the pure LN are six coordinated, as shown in figure 1, Li will have bonds of valence 1/6 and Nb bonds of valence 5/6. The environment of Mg in oxygen-containing compounds is nearly the same as that of Li: six coordinate, and with similar bond lengths [24]; therefore, Mg would have bonds of $2/6 = 1/3$ in the host frame. In $LiNbO_3$ each O atom receives two bonds from Nb and two from Li, giving a valence sum of $2(5/6) + 2(1/6) = 2.00$. If one substituted Mg for Li completely, one would have the compound $MgNb_2O_6$ in which half the Li sites would be vacant. In this case, the O atoms would receive $2(5/6) + 1(1/3) = 2.00$. Mg-doped LN single crystals can be regarded as a mixture of the two cases; their crystal formula can be written as $(LiNbO_3)(1 - x)\cdot(MgNb_2O_6)(x/2)$. This 'mixed case' will be the basis for all of the following calculations.

3. Theoretical method

The two compounds which build up the doped crystal considered here are each decomposed into a sum of single bonds according to their respective bonding situations, yielding the bond-valence equations

$$\mathrm{LiNbO_3} = \frac{1}{2}\mathrm{LiO(l)}_{3/2} + \frac{1}{2}\mathrm{LiO(s)}_{3/2} + \frac{1}{2}\mathrm{NbO(l)}_{3/2} + \frac{1}{2}\mathrm{NbO(s)}_{3/2} \tag{3}$$

$$\mathrm{MgNb_2O_6} = \frac{1}{2}\mathrm{MgO(l)}_2 + \frac{1}{2}\mathrm{MgO(s)}_2 + \mathrm{NbO(l)}_2 + \mathrm{NbO(s)}_2. \tag{4}$$

As shown in the previous work [17], the chemical bond method regards certain macroscopic physical properties of a crystal as combinations of the contributions of all constituent chemical bonds. According to the relationship between the crystal structure and the dielectric response of crystal materials, the linear and second-order nonlinear optical properties of any crystal can be calculated using the appropriate geometric sum of the respective properties of its corresponding constituent chemical bonds. On the basis of the crystallographic structure of a given crystal, its linear and second-order nonlinear optical susceptibilities χ and d_{ij} can thus be written as

$$\chi = \sum_{\mu} F^{\mu}\chi^{\mu} = \sum_{\mu} N_b^{\mu}\chi_b^{\mu} \tag{5}$$

and

$$d_{ij} = \sum_{\mu}\left\{\frac{G_{ij}^{\mu}N_b^{\mu}(0.5)\left\{\left[(Z_{\mathrm{A}}^{\mu})^* + n(Z_{\mathrm{B}}^{\mu})^*\right]/\left[(Z_{\mathrm{A}}^{\mu})^* - n(Z_{\mathrm{B}}^{\mu})^*\right]\right\} f_i^{\mu}(\chi_b^{\mu})^2}{d^{\mu}q^{\mu}} + \frac{G_{ij}^{\mu}N_b^{\mu}s(2s-1)\left[r_0^{\mu}/(r_0^{\mu}-r_c^{\mu})\right]^2 f_c^{\mu}(\chi_b^{\mu})^2\rho^{\mu}}{d^{\mu}q^{\mu}}\right\} \tag{6}$$

respectively. Parameters used in equations (5) and (6), and in tables 1 and 2, include:

F^{μ}:	fraction of bonds of type μ composing the crystal.
χ^{μ}:	linear susceptibility contribution from μ-type bonds.
N_b^{μ}:	number of bonds of type μ per cm^3.
χ_b^{μ}:	susceptibility of a single bond of type μ.
G_{ij}^{μ}:	geometrical contribution of chemical bonds of type μ.
$(Z_{\mathrm{A}}^{\mu})^*$, $(Z_{\mathrm{B}}^{\mu})^*$:	effective number of valence electrons of A and B ions, respectively.
n:	ratio of numbers of the two elements B and A in the bond-valence equation [18].
f_i^{μ}, f_c^{μ}:	fractions of ionic and covalent characteristics of the individual bonds, $f_i^{\mu} = (C^{\mu})^2/[(E_h^{\mu})^2 + (C^{\mu})^2]$ and $f_c^{\mu} = 1 - f_i^{\mu}$, where C^{μ}, E_h^{μ} are the average energy gaps due to ionic and covalent effects.
d^{μ}:	bond length of the μ-type bonds in Å.
q^{μ}:	bond charge of the μth bond.
s:	exponent in the bond force constant.
$r_c^{\mu} = 0.35r_0^{\mu}$:	core radius, where $r_0^{\mu} = d^{\mu}/2$ and d^{μ} is the bond length.
$\rho^{\mu} = (r_{\mathrm{A}}^{\mu} - r_{\mathrm{B}}^{\mu})/(r_{\mathrm{A}}^{\mu} + r_{\mathrm{B}}^{\mu})$:	difference in the atomic sizes, where r_{A}^{μ} and r_{B}^{μ} are the covalent radii of atoms A and B, taken from the periodic table of elements.

Table 1. Calculated chemical bond parameters: linear and second-order nonlinear optical properties of selected constituent bonds in pure $LiNbO_3$ single crystals at 1079 nm.

	Li–O(l)	Li–O(s)	Nb–O(l)	Nb–O(s)
d^μ (Å)	2.245	2.063	2.130	1.876
f_c^μ	0.649	0.666	0.220	0.226
χ^μ	3.132	2.705	5.603	4.475
q^μ/e	0.180	0.199	0.536	0.641
G_{22}^μ	−0.027	−0.014	−0.032	0.065
d_{22}^μ (pm V^{-1})	2.029	0.775	0.201	−0.292
G_{31}^μ	0.176	−0.152	−0.184	0.183
d_{31}^μ (pm V^{-1})	−13.015	8.559	1.152	−0.826
G_{33}^μ	0.360	−0.041	−0.303	0.103
d_{33}^μ (pm V^{-1})	−26.682	2.322	1.892	−0.466

Table 2. Calculated chemical bond parameters: linear and second-order nonlinear optical properties of selected constituent bonds in the structural unit $MgNb_2O_6$ of Mg-doped $LiNbO_3$ single crystals at 1079 nm.

	Mg–O(l)	Mg–O(s)	Nb–O(l)	Nb–O(s)
d^μ (Å)	2.245	2.063	2.130	1.876
f_c^μ	0.473	0.488	0.237	0.248
χ^μ	3.359	2.924	4.656	3.766
q^μ/e	0.322	0.356	0.609	0.720
G_{22}^μ	−0.027	−0.014	−0.032	0.065
d_{22}^μ (pm V^{-1})	0.739	0.291	0.329	−0.497
G_{31}^μ	0.176	−0.152	−0.184	0.183
d_{31}^μ (pm V^{-1})	−4.738	3.215	1.887	−1.408
G_{33}^μ	0.360	−0.041	−0.303	0.103
d_{33}^μ (pm V^{-1})	−9.713	0.872	3.100	−0.795

According to Levine's model [25] the susceptibility χ^μ of any bond of type μ can be expressed as

$$\chi^\mu = (4\pi)^{-1}(\hbar\Omega_p^\mu)^2/\left[(E_h^\mu)^2 + (C^\mu)^2\right] \tag{7}$$

where Ω_p^μ is the plasma frequency. The average covalent energy gap E_h^μ of a bond is given by [26, 27]

$$E_h^\mu = 39.74/(d^\mu)^s \qquad s = 2.48 \tag{8}$$

and the average ionic gap C^μ by

$$C^\mu = b^\mu \exp(-k_s^\mu r_0^\mu)[(Z_{\mathrm{A}}^\mu)^* - nZ_{\mathrm{B}}^\mu)^*]/r_0^\mu \tag{9}$$

where $\exp(-k_s^\mu r_0^\mu)$ is the Thomas–Fermi screening factor and b^μ is a correction factor of order unity [26] taking into account the more complex true screening behaviour in crystals.

The bond charge q^μ can be expressed as [17, 18]

$$q^\mu = (n_e^\mu)^*\left[1/(\chi^\mu + 1) + f_c^\mu(2^{F_c} - 1.1)/N_{\mathrm{cation}}\right]e \tag{10}$$

where $(n_e^\mu)^*$ is the number of valence electrons per bond μ, $F_c = \sum_\mu N_b^\mu f_c^\mu$ is the crystal covalency, and N_{cation} is the cation coordination number.

The geometrical factors G_{ij}^μ for the contributions of the respective bond types μ to the tensor coefficients d_{ij} are deduced from the crystal geometry:

$$G_{ij}^\mu = G_{ikl}^\mu = (1/n_b^\mu) \sum_\lambda \alpha_{i,\lambda}^\mu \alpha_{k,\lambda}^\mu \alpha_{l,\lambda}^\mu. \tag{11}$$

The sum on λ is to be taken over all n_b^μ symmetry-equivalent bonds of type μ in the unit cell. $\alpha_{i,\lambda}^\mu$ denotes the direction cosine of the λth bond of type μ in the unit cell with respect to the ith axis of the optical indicatrix; ij is the contracted form of the full set of indices ikl used in the third-rank nonlinear susceptibility tensor.

4. Results and discussion

According to the detailed chemical bonding situations of constituent Li, Nb, and O atoms, which are obtained from the detailed crystallographic data of LN [28], we can calculate chemical bond parameters: linear and second-order nonlinear optical properties of constituent Li–O and Nb–O bonds at 1079 nm, respectively. Then the contributions of these constituent chemical bonds (and further LiO_6 and NbO_6 clusters) to the total linear and second-order nonlinear optical responses of the whole crystal can be quantitatively determined. These results are listed in table 1. According to our constructed structure–property relationship, we can make calculations for the case of Mg-doped LN. According to our assumptions described above, there are two structural units in Mg-doped LN single crystals: $LiNbO_3$ and $MgNb_2O_6$ in the ratio $(1 - x)/(x/2)$. The calculated results for the $MgNb_2O_6$ part are listed in table 2, from which we can find the influence of doped Mg^{2+} cations on the microscopic chemical bonding environments of Nb^{5+} cations.

Using these results for the individual bond susceptibilities, we can quantitatively calculate all independent second-order NLO tensor coefficients d_{22}, d_{31}, and d_{33} at 1079 nm of the pure and Mg-doped LN single crystals with various compositions. The calculated numerical values for pure LN are $d_{22} = 2.713$ pm V^{-1}, $d_{31} = -4.130$ pm V^{-1}, and $d_{33} = -22.934$ pm V^{-1}. These results agree well with the reported experimental data at 1064 nm [29]: $d_{22} = 2.1$ pm V^{-1}, $d_{31} = -4.3$ pm V^{-1}, and $d_{33} = -27$ pm V^{-1}, as well as with our previously calculated results for 1064 nm [18]. In the present calculation, data for the ordinary refractive indices n_o at 1079 nm for pure and Mg-doped LN crystals (data derived from the generalized Sellmeier equation taken from reference [16]) are used as reference values to determine the global correction factor b^μ used in equation (9) as an addition to the Thomas–Fermi screening factor. This is necessary to get a good accuracy for the calculation of the nonlinear properties.

All calculated results for pure LN and Mg-doped LN at various doping levels are plotted in figure 4. The influence of the Mg doping can be clearly stated: the nonlinear optical response of the material decreases linearly with increasing doping level. This is the same tendency, yet more strongly expressed, as is found for the linear optical response [16]. Our current results agree quantitatively with the reported observation of the reduction of the tensor coefficient d_{31} of Mg-doped LN, which is only 79% of that of pure LN [30].

From the current work, we can conclude that the dielectric responses (including refractive indices and second-order NLO responses) of LN crystals are very sensitive to the doped Mg^{2+} cations at Li sites. This is in agreement with our previous conclusions that in the LN crystallographic frame the Li sites are the sensitive crystal lattice sites [17,18], at which dopants can modify the dielectric properties of LN crystals most effectively. That may be one of the

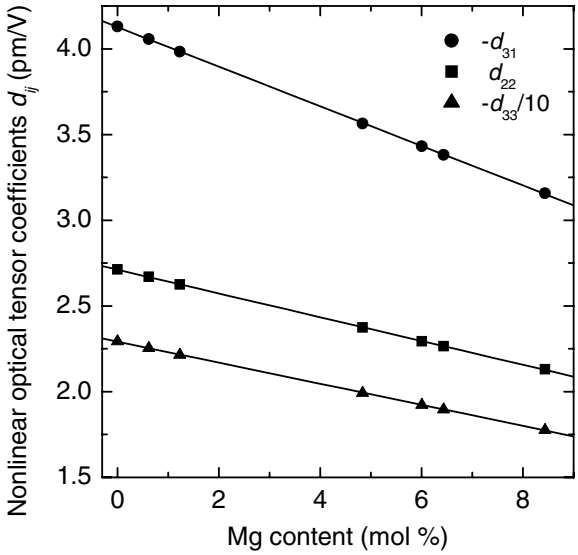

Figure 4. Dependences of the second-order nonlinear optical tensor coefficients d_{ij} of Mg-doped $LiNbO_3$ crystals at 1.079 μm on the Mg concentration in the crystal.

reasons for the versatility of lithium niobate obtained by introducing dopants at Li sites in the crystallographic frame.

5. Conclusions

From the chemical bond viewpoint for crystal materials, we have studied second-order NLO properties of the Mg-doped LN crystals, at 1079 nm. The present work shows us that the second-order NLO response of the Mg-doped LN crystals decreases with increasing Mg content in the crystal lattice. We can also conclude that in LN crystals, the Li sites are the sensitive crystal lattice sites, at which dopants can affect the dielectric properties of LN crystals most effectively. Therefore, dielectric properties of LN crystals can be considerably modified by introducing various suitable dopants at Li sites.

Acknowledgments

Dr Xue thanks the Alexander von Humboldt Foundation for support during his stay in Germany. The first author also thanks Professor I D Brown for kindly clarifying aspects of the bond-valence model and many helpful discussions on the current work.

References

[1] Räuber A 1978 *Current Topics in Materials Sciences* ed E Kaldis (Amsterdam: North-Holland)
[2] Krätzig E and Schirmer O F 1988 *Photorefractive Materials and Their Applications* ed P Günter and J P Huignard (Berlin: Springer)
[3] Abrahams S C and Marsh P 1986 *Acta Crystallogr.* B **42** 61
[4] Malovichko G, Grachev V and Schirmer O 1999 *Appl. Phys.* B **68** 785
[5] Safaryan F P, Feigelson R S and Petrosyan A M 1999 *J. Appl. Phys.* **85** 8079
[6] Lorenzo A, Jaffrezic H, Roux B, Boulon G and Garcia-Sole J 1995 *Appl. Phys. Lett.* **67** 3735

[7] Johnson L F and Ballman A A 1969 *J. Appl. Phys.* **40** 297
[8] Volk T, Wöhlecke M, Rubinina N, Reichert A and Razumovski N 1996 *Ferroelectrics* **183** 291
[9] Zhong G, Jin J and Wu Z 1980 *Proc. 11th Int. Quantum Electronics Conf.* Cat. No 80CH1561-0 (New York: IEEE) p 631
[10] Bryan D A, Gerson R and Tomaschke H E 1984 *Appl. Phys. Lett.* **44** 847
[11] Wilkinson A P, Cheetham A K and Jarman R H 1993 *J. Appl. Phys.* **74** 3080
[12] Zotov N, Boysen H, Frey F, Metzger T and Born E 1994 *J. Phys. Chem. Solids* **55** 145
[13] Donnerberg H, Tomlinson S M, Catlow C R A and Schirmer O F 1991 *Phys. Rev.* B **44** 4877
[14] Shimamura S, Watanabe Y, Sota T, Suzuki K, Iyi N, Yajima Y, Kitamura K, Yamazaki T, Sugimoto A and Yamagishi K 1996 *J. Phys.: Condens. Matter* **8** 6825
[15] Iyi N, Kitamura K, Yajima Y, Kimura S, Furukawa Y and Sato M 1995 *J. Solid State Chem.* **118** 148
[16] Schlarb U and Betzler K 1994 *Phys. Rev.* **50** 751
[17] Xue D and Zhang S 1999 *Physica* B **262** 78
[18] Xue D and Zhang S 1997 *J. Phys.: Condens. Matter* **9** 7515
[19] Brown I D 1992 *Acta Crystallogr.* B **48** 553
[20] Xue D, Betzler K, Hesse H and Lammers D 1999 *Phys. Status Solidi* b **216** R7
[21] Rosner W, Grabmaier B and Wersing W 1989 *Ferroelectrics* **93** 57
[22] Schirmer O F, Thiemann O and Wöhlecke M 1991 *J. Phys. Chem. Solids* **52** 185
[23] Grabmaier B, Wersing W and Koestler W 1991 *J. Cryst. Growth* **110** 339
[24] Blatov V A, Pogildyakova L V and Serezhkin V N 1999 *Acta Crystallogr.* B **55** 139
[25] Levine B F 1973 *Phys. Rev.* B **7** 2600
[26] Levine B F 1973 *Phys. Rev.* B **7** 2591
[27] Van Vechten J A 1969 *Phys. Rev.* **182** 891
[28] Hsu R, Maslen E N, Boulay D and Ishizawa N 1997 *Acta Crystallogr.* B **53** 420
[29] Roberts D A 1992 *IEEE J. Quantum Electron.* **28** 2057
[30] Eckardt R C, Masuda H, Fan Y X and Byer R L 1990 *IEEE J. Quantum Electron.* **26** 922